Available online at www.sciencedirect.com
ScienceDirect
Talanta 74 (2008) 944–950
Talanta
www.elsevier.com/locate/talanta

Studies of the interaction between Aloe-emodin and DNA and preparation of DNA biosensor for detection of PML-RARα fusion gene in acute promyelocytic leukemia

Xin Hua Lin [a,*], Hong Yan Wan [a,*], Ya Feng Zhang [b], Jing Hua Chen [a]

[a] *Department of Pharmaceutical Analysis, Faculty of Pharmacy, Fujian Medical University, Fuzhou 350004, PR China*
[b] *Xi'an Institute for Drug Control, Xi'an 710054, PR China*

Received 19 March 2007; received in revised form 29 July 2007; accepted 30 July 2007
Available online 14 August 2007

Abstract

The interaction of Aloe-emodin (AE) with salmon sperm DNA in 0.1 M Tris–HCl buffer (pH 4.4) and at the DNA-modified glassy carbon electrode (GCE) was systemically studied with voltammetry and ultraviolet–visible (UV–vis) spectroscopy. AE had excellent electrochemical activity on the GCE with a couple of redox peaks. We propose that AE can intercalate into DNA strands forming a nonelectroactive complex, which results in the decrease of the reduction peak current of AE. The Langmuir adsorption constants of AE at ss- and dsDNA/GCE were $(2.1 \pm 0.4) \times 10^5$ and $(2.7 \pm 0.2) \times 10^5$ M^{-1}, respectively. The difference between AE at ss- and dsDNA has been used for the preparation of a sequence-specific DNA electrochemical biosensor for detection of PML-RARα fusion gene in acute promyelocytic leukemia (APL) with a detection limit of 6.7×10^{-8} M and a linear range from 1.5×10^{-8} to 1.5×10^{-7} M. The selectivity of ssDNA-modified electrode was also described.

Keywords: Aloe-emodin; Salmon sperm DNA; Interaction; Voltammetry; APL; DNA electrochemical biosensor

1. Introduction

DNA biosensors based on nucleic acid hybridization are currently under intense investigation owing to their increasing importance in the diagnosis of disease with low cost and low power requirements [1–3]. These sensors can be prepared by immobilizing single-stranded DNA probes on the surface of different electrodes. These devices can be used to detect sequence-specific hybridization events directly [4] or by DNA intercalators (anticancer agents [5,6], organic dyes [7,8], and metal complexes [9,10], etc.), which form complexes with the nitrogenous bases of DNA.

The interaction of DNA with small molecules represents a fundamental issue in life science and has been the subject of several investigations [11,12]. The small molecules which noncovalently interact with DNA, are stabilized in binding to DNA through a series of weak interactions, such as the π-stacking interactions associated with intercalation of aromatic heterocyclic groups between the base pairs, hydrogen-bonding, and van der Waals interactions of functionalities bound along the groove of the DNA helix. It would be valuable to understand quantitatively the contributions from these different modes to stabilization of the bound complex at a DNA site [13]. Aloe-emodin (1,8-dihydroy-3-[hydroxymethyl]-anthraquione), a bioactive anthraquinone from the root and rhizome of *Rheum palmatum* L. (Polygonaceae) [14], has been found to have antitumor, genotoxicity, antioxidation, and antibacterial effects [15–18]. The interaction of anthraquinone derivatives with DNA was reported. McKnight et al. [19] studied the DNA binding characteristics of a series of homologous 2, 6-disubstituted anthraquinone threading intercalators. They found that the binding constant decreased with the increase of the side chain length. Bi et al. [20] investigated the anthraquinones such as emodin, rhein, aloe-emodin, and aloin binding properties with serum albumin (BSA or HSA) by fluorescence quenching and absorption spectroscopic techniques. It has been revealed that there were relatively strong binding affinity for the four anthraquinones with HSA and BSA. To our knowledge, there are no reports on detailed investigation of the

* Corresponding authors. Tel.: +86 591 22862016; fax: +86 591 22862016.
E-mail addresses: xinhua63@163.com (X.H. Lin), whypolaris@126.com (H.Y. Wan).

0039-9140/$ – see front matter © 2007 Elsevier B.V. All rights reserved.
doi:10.1016/j.talanta.2007.07.038

interaction mechanism of AE with ss- and dsDNA by voltammetry.

Acute promyelocytic leukemia (APL) accounts for about 5–15% of all acute myeloid leukemias and is characterized by the chromosomal translocation t(15;17), which fuses the retinoic acid receptor (RAR) α gene to the promyelocytic leukemia (PML) gene[21,22]. The PML-RARα fusion gene plays an important role in leukemogenesis through antagonizing retinoic acid signalling and the regulatory pathways mediated by PML. The availability of genotype-specific therapy for PML/RARα acute promyelocytic leukemia requires a precise diagnosis of the disease and DNA biosensors can provide a rapid, precise, and sensitive means for disease diagnosis.

In this paper, we investigated the interactions of AE with DNA in solutions and at ss- and dsDNA-modified GCE. The intercalative binding of AE with DNA forms a nonelectroactive supramolecular complex. In addition, based on the peak current change in electrochemical measurements, a sequence-specific DNA electrochemical sensor for detection of PML-RARα fusion gene in APL was prepared. It was developed by immobilizing covalently single-stranded PML-RARα DNA fragments to a modified GCE. The surface hybridization of the immobilized single-stranded PML-RARα gene fragment with its complementary DNA fragment was evidenced using AE as a novel electrochemical indicator with a detection limit of 6.7×10^{-8} M and the selectivity of ssDNA-modified electrode was also described. This will bring further insight about the interaction mechanism between AE and DNA, and is helpful for further research to design novel antitumor drugs and diagnosis disease.

2. Experimental

2.1. Apparatus

Cyclic voltammograms (CVs) and differential pulse voltammograms (DPVs) were recorded on an electrochemical workstation 660B (CH Instrument, China). A conventional three-electrode system was used throughout the experiments. A GCE (3 mm diameter) was used as the working electrode, a twisted platinum wire as auxiliary electrode, and an Ag/AgCl (with saturated KCl) electrode as the reference electrode. UV–vis absorbance spectra were measured with a UV-2501PC spectrophotometer (SHIMADZU, Japan) using a quartz cell having 1.0 cm optical pathway.

2.2. Reagents

The 18-base synthetic oligonucleotides were purchased from Shanghai Chemical Reagents Company (China); their base sequences are as follows:

- immobilized probe(18-base sequence S_1)-5′-NH3 TCT CAA TGG CTG CCT CCC-3′;
- target (18-base sequence S_2)-5′-GGG AGG CAG CCA TTG AGA-3′;
- single-base mismatch (18-base sequence S_3)-5′-GGG AAG CAG CCA TTG AGA-3′;
- non-complementary (18-base sequence S_4)-5′-ACG TGG TCC CCA GCT CTC-3′.

All oligonucleotides stock solutions (100 μg/mL) were prepared with TE solution (10 mM Tris–HCl, 1.0 mM EDTA, and pH 8.00) and kept frozen. More dilute solutions were prepared with 20 mM acetate buffer (pH 4.80). Salmon sperm DNA was obtained from Aldrich and used as received. Real samples were kindly donated by Fujian institute of hematology, the affiliated union hospital of Fujian medical university. Stock solutions of salmon sperm DNA (1.0 mg/mL) were prepared by dissolving nucleic acids in a 0.1 M Tris–HCl buffer (pH 7.0) and stored at 4 °C. Denatured ssDNA was produced by heating a dsDNA solution in a water bath at 100 °C for 5 min, immediately followed by rapid cooling in an ice bath. Aloe-emodin was purchased from National Institute for the control of pharmaceutical and biological products (China). It was dissolved in ethanol and stored in the dark. *N*-hydroxysulfosuccinimide and *N*-(3-dimethylamion)propyl-*N*′-ethyl carbodiimidehydrochloride were obtained from Sigma. The stock solution of 5 mM DEC and 8 mM NHS was prepared in 50 mM phosphate buffer solutions (PBS, pH 7.40). All the buffer solutions contained 20 mM NaCl. Other chemicals were of analytical reagent grade. All solutions were prepared with double-distilled water (DDW).

2.3. Electrochemical study on the interaction between AE and DNA

2.3.1. Interaction of AE with different concentration of dsDNA

Twenty microliters of 1.0×10^{-3} M AE solution was transferred into 10 mL volumetric flask containing 100, 200 or 400 μL salmon sperm dsDNA stock solution. Each mixture was diluted to the mark using 0.1 M Tris–HCl buffer (pH 4.4). The test solution was subsequently placed in the cell and deaerated with highly pure nitrogen for 3 min prior to measurements. After that, the electrode was placed into the test solution and for CV and DPV scans after adequately stirred for 180 s at open circuit.

2.3.2. Interaction of AE with ss- or dsDNA in solution

Two-hundred microliters of salmon sperm ss- or dsDNA stock solution was transferred into 10 mL volumetric flask and then it was mixed with 20 μL of 1.0×10^{-3} M AE solution. Each mixture was diluted to the mark using Tris–HCl buffer (pH 4.4). The following procedure was the same as above.

2.3.3. Binding constants of AE to ss- or dsDNA-modified electrode

The GCE was mechanically polished with 0.05 μM Al_2O_3 slurry, and then washed ultrasonically in water followed by ethanol for a few minutes. Afterwards, the electrode was oxidized at 0.5 V for 1 min in 50 mM PBS (pH 7.40), followed by

thorough rinse with DDW. Salmon sperm ssDNA (1.0 mg/mL and 10 μL) was pipetted onto the GCE surface. After air-drying, the electrode was rinsed with distilled water. The dsDNA-modified GCE was prepared by dropping salmon sperm dsDNA instead of ssDNA on the GCE surface. The modified electrode was immersed in 2.0×10^{-6} M AE solution for 6 min and then was transfered to blank Tris–HCl buffer (pH 4.4) which had been deaerated with highly pure nitrogen for 3 min for DPV scans.

2.4. UV–vis absorbance spectroscopic studies of the interaction between AE and ss- or dsDNA

Volumes of 1.0 mL Tris–HCl buffer and 100 μL AE solution were transferred into a 5 mL volumetric flask. 200 μL of salmon sperm ss- or dsDNA DNA stock solution was also added. The above solutions were then mixed, diluted to the volume with Tris–HCl buffer (pH 4.4) and mixed thoroughly. Then UV–vis absorbance spectra was measured after leaving the mixture at room temperature for 90 min. Pure AE solution was prepared in a similar manner without DNA.

2.5. Preparation of the electrochemical DNA biosensor

The electrochemical DNA biosensor developed was based on the covalent immobilization of ssDNA on the modified electrode. Modification of the electrode was achieved by dropping 20 μL solution containing 5 mM DEC and 8 mM NHS in 50 mM PBS. After the solution was air-dried, the fabricated electrode was rinsed with DDW for several times. Subsequently, 10 μL ssDNA solution (S_1) was dropped on the modified GCE surface and air-dried to dryness. Then the electrode was rinsed with DDW to eliminate the DNA adsorbed.

2.6. Electrochemical detection of the target-specific DNA hybridization

To achieve the DNA interaction, the S_1-immobilized electrode was immersed in pH 7.0 Tris–HCl buffer containing complementary S_2, single-base mismatch S_3 and non-complementary S_4, respectively. The hybridization was allowed for 30 min at 45 °C. Afterwards, the electrode was dried at room temperature and then thoroughly rinsed with the same Tris–HCl buffer and DDW successively to eliminate the adsorbed S_2, S_3, and S_4.

For DPV detection of the DNA hybridization, AE was used as a hybridization indicator. To accumulate AE on the electrode surface, S_1-immobilized GCE and the modified electrodes obtained after hybridization with complementary S_2, single-base mismatch S_3 or non-complementary S_4 were immersed in Tris–HCl buffer (pH 4.4) containing 2.0×10^{-6} M AE for 6 min at room temperature. Then, the electrodes were rinsed with the PBS and DDW successively. After this modified electrode was transferred into the blank Tris–HCl buffer which had been deaerated with highly pure nitrogen for 3 min, DPV were collected from −0.1 to −0.8 V with amplitude of 10 mV at 50 mV/s scan rate.

2.7. Hybridization detection in real samples

cDNA was obtained by applying a reverse transcription method from total RNA which was extracted using mini DNA-free total RNA extraction kit from venous blood as described previously [23]. The hybridization detection of real samples was transduced by means of DPV. The procedure of hybridization detection of the real samples consisted of the following steps. GCE pretreatment, probe immobilization, and hybridization with DNA fragments obtained from venous blood by using the same electrode surface, indicator binding, and voltammetric transduction of the electrode surface.

3. Results and discussion

3.1. Interaction of AE with dsDNA in solution

As shown in Fig. 1 (curve a), upon the addition of 2.0×10^{-6} M AE to Tris–HCl buffer, a couple of reversible redox peaks appeared with anodic and cathodic peak potentials at about −429 and −456 mV, respectively. Note that the anodic peak was smaller compared to the cathodic peak. As the pH value was increased, the anodic peak disappeared, while the cathodic peak increased. Therefore, the cathodic peak was chosen as the focus for the following investigation. The reduction peak current obtained for AE showed linear dependence on the scan rate, suggesting the adsorption of AE on the electrode surface. The linear equation was: $y = 0.0153x + 2.0582$; $r = 0.9998$. The pH value plays an important role in the electrochemical behavior of AE and AE–DNA complex. With the pH value of the solution increasing, the peak potential shifted to more negative values and the peak currents changed significantly. In the pH range from 3.0 to 7.4, the relation between peak potential and pH was directly investigated and the linear regression equations, $E^{\circ\prime}$ (mV) = −50.26 and pH 247.4 ($r = 0.9966$) for AE and $E^{\circ\prime}$ (mV) = −47.60 and pH 264.8 ($r = 0.9943$) for AE–DNA complex, were obtained. This showed that the uptake of electrons was accompanied by an equal number of protons [24,25], indepen-

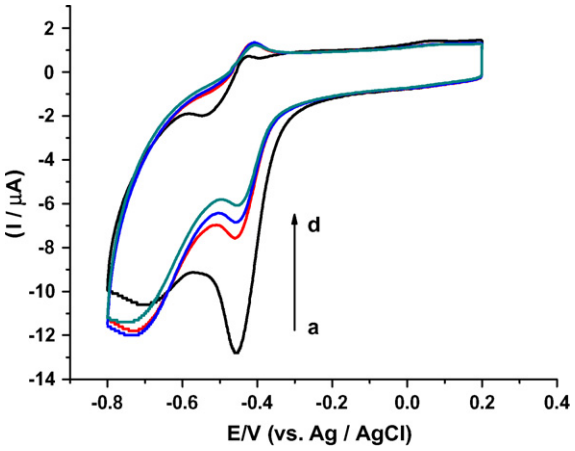

Fig. 1. CVs for 2.0×10^{-6} M AE in the absence (curve a) and presence of 3.1×10^{-5} M (curve b), 6.2×10^{-5} M (curve c), and 1.2×10^{-4} M dsDNA (curve d). Scan rate: 100 mV/s; scan range: 0.2 V to −0.8 V; rest time: 2 s.

dent of the presence of DNA. For a reversible adsorption peak [26], the value of peak separation (ΔE_p) is 58/n mV at 25 °C. For the couple of redox peaks of AE and AE–DNA complex, ΔE_p were 27 and 32 mV, respectively. Thus, the estimated numbers of electrons transferred during the electrode reaction were 2 in both cases. So it can be concluded that, no matter whether DNA is present or not, the electrode reaction processes are both two-electron transfer with two-proton uptake.

Cyclic voltammograms of AE in the absence and presence of DNA were shown in Fig. 1. As can be seen, the decrease of peak current was also observed with increasing of DNA. The reduction peak current (I_{pc}) of AE decreased and the peak potentials did not change. The binding equilibrium time during which AE was in contact with DNA had a great influence on both the stability of the peak and the decrease in peak current. With increased the soaking time of the electrode in AE–DNA complex solution, the peak current decreased and then trended to a steady value. So a time of 6 min was the optimal waiting time.

The phenomena mentioned above were further studied by DPV. The decrease of peak current was also observed with increasing of DNA. As far as ΔI_{pc} was concerned, it was found to be in linear proportion to the concentration of DNA in the range of 1.86×10^{-5} to 1.12×10^{-4} M with a regression equation $\Delta I_{pc} = 0.0079 C_{DNA} + 2.0 \times 10^{-6}$, and a correlation coefficient $r = 0.9992$.

The possible reason for the decrease of the peak current after addition of DNA to AE solution is that the presence of DNA may alter the electrochemical kinetics of AE. The values of the major electrochemical kinetic parameters of AE in the absence and the presence of dsDNA can indicate whether the presence of DNA influences the electrochemical kinetics of AE. The electron transfer coefficient α and the standard rate constant k_s can be determined via the theory of Laviron [27]. A graph of $E_{pc} = f(\log v)$ yields a straight line with a slope equal to $-2.3RT/\alpha nF$ for the cathodic peak, where v stands for the scan rate, n the number of electrons, and R, T, and F have their normal meanings. Plotting E_{pc} versus log v produces a linear range, so α has been estimated to be 0.24 for the AE redox reaction in the absence of dsDNA. k_s can be calculated according to the following equation (valid when $n\Delta E_p > 200$ mV):

$$\log k_s = \alpha \log(1-\alpha) + (1-\alpha)\log\alpha - \log\frac{RT}{nFv} - \frac{\alpha(1-\alpha)nF\Delta E_p}{2.3RT} \quad (1)$$

from which k_s has been determined to be 12.40 s^{-1} (at a scan rate of 100 mV/s). Similarly, α and k_s for the AE redox reactions in the presence of dsDNA have been calculated to be 0.20 and 10.35 s^{-1}, respectively. Obviously, the presence of dsDNA does not significantly alter the kinetics of the AE redox reactions at the GCE surface. From the results above it can be assumed that there is a binding and complexation between AE and DNA. Because of the interaction between AE and DNA, an electrochemically inactive complex forms according to the Ref. [28], the AE–DNA complex, which cannot be oxidized at the electrode surface.

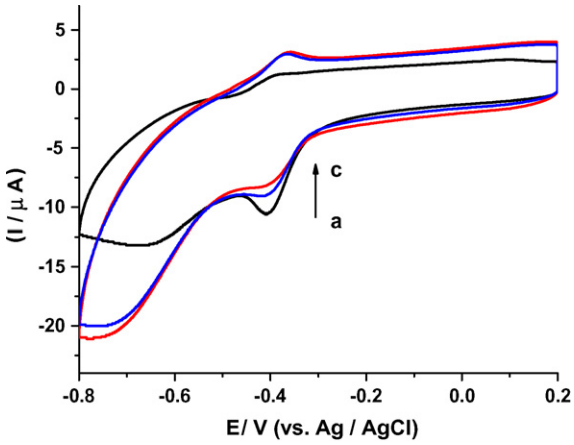

Fig. 2. CVs for 2.0×10^{-6} M AE in the absence (curve a), presence of 6.2×10^{-5} M ssDNA (curve b), and 6.2×10^{-5} M dsDNA (curve c). Other conditions as Fig. 1.

3.2. Interaction of AE with dsDNA or ssDNA in solution

The different electrochemical behaviors of AE with the addition of dsDNA or ssDNA in the buffer solution also demonstrate the interaction between AE and DNA. As shown in Fig. 2, although the peak current of AE decreases in both cases, the peak current decreases more sharply at dsDNA-modified electrode.

The UV–vis absorption spectrum also provides potent evidence for the possible intercalation of AE into DNA. As shown in Fig. 3, although a slight shift in the AE adsorption peak from 407 to 414 nm is observed after the addition of dsDNA, the absorption peak decreases significantly. In contrast with dsDNA, the absorption peak of denatured ssDNA decreases slightly. These phenomena suggest the possible intercalation of AE into dsDNA strands [29–31]. The studies described above indicated that upon binding to DNA the planar anthraquinone ring of AE could slide into adjacent base pairs [32], resulting in that they were in an environment in which it was unable to H bond with the solvent water molecules. In contrast, the random coil-like, disordered ssDNA does not provide a favorable environment for AE intercalation.

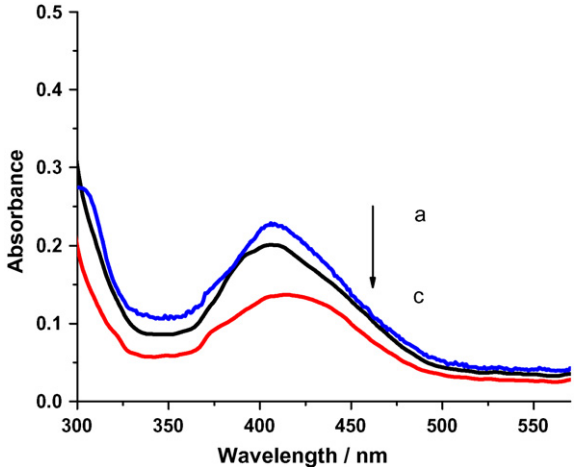

Fig. 3. UV–vis absorption spectrum for 2.0×10^{-5} M AE in the absence (curve a) and presence of 40.0 μg mL^{-1} M ssDNA (curve b) and dsDNA (curve c).

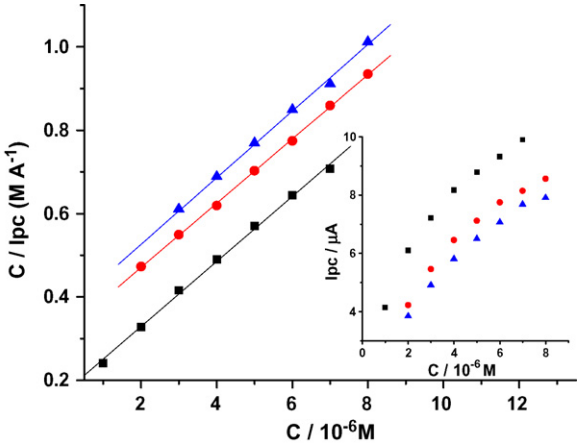

Fig. 4. Plots of C/I_{pc} vs. AE concentration at bare GCE (■), salmon sperm dsDNA/GCE (●) and salmon sperm ssDNA/GCE (▲). Inset: relations between cathodic peak currents and AE concentration. The scan rate, pulse amplitude, and pulse period were 20 mV/s, 50 mV, and 60 ms, respectively.

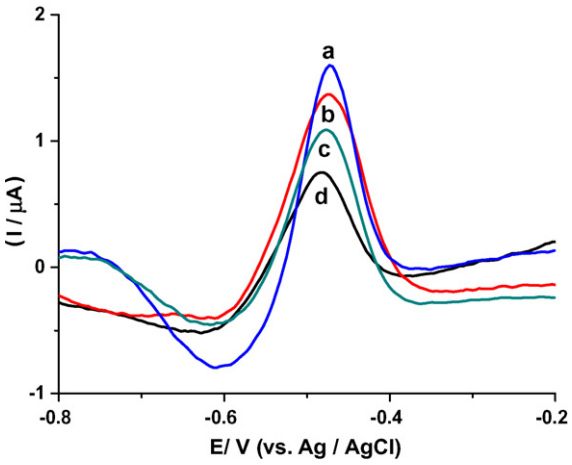

Fig. 5. DPVs of AE accumulated on the bare GCE (curve a), ssDNA modified GCE (curve d) and after hybridization with non-complementary sequence (curve c), and complementary sequence (curve b) in a 0.1 M Tris–HCl buffer (pH 4.40) with 20 mM NaCl. Other conditions as Fig. 4.

3.3. Binding constants of AE to dsDNA/GCE and ssDNA/GCE

The cyclic voltammograms of AE at different concentrations at bare GCE, ss- or dsDNA/GCE electrodes showed that the peak current increased with increasing AE concentration, as expected shape of Langmuir adsorption [33] (Fig. 4). Thus, the adsorption thermodynamics is given in the following equation:

$$\frac{C}{I_p} = \frac{1}{KI_{p,max}} + \frac{C}{I_{p,max}} \quad (2)$$

where I_p, $I_{p,max}$, C, and K are the peak current, maximum peak current, AE concentration, and the adsorption or binding constant of AE at bare GCE, ss- or dsDNA/GCE surface. From the slope and intercept of C/I_p versus C the maximum peak current, $I_{p,max}$, and the adsorption constant, K, can be obtained.

Fig. 4 shows the plots of C/I_p versus C at three electrodes. From the linear regression equation, the adsorption constants of AE at bare glass carbon electrode and the binding constant of AE to ssDNA/GCE and dsDNA/GCE at pH 4.4 were calculated to be $(4.5 \pm 0.2) \times 10^5$, $(2.1 \pm 0.4) \times 10^5$ and $(2.7 \pm 0.2) \times 10^5$ M^{-1}, respectively. The adsorption constant of AE at bare electrode is much larger than the binding constant of AE to ssDNA/GCE and dsDNA/GCE, which indicated that an intense adsorption process of AE on the electrode surface. Although the amount of adsorbed ssDNA is more than that of adsorbed dsDNA, the dsDNA/GCE shows a larger peak current of AE and a larger binding constant. Under the same conditions, the larger binding constant of AE to dsDNA/GCE than to ssDNA/GCE indicates that AE can be used as a novel electroactive indicator for detection of DNA hybridization.

3.4. Electrochemical detection of the target-specific DNA hybridization

Since AE could intercalate into the bases of dsDNA, the DNA biosensor using AE as electrochemical hybridization label was developed. The selectivity of the electrochemical DNA sensor developed was studied using DPV. Fig. 5 shows the DPV curves obtained in blank Tris–HCl buffer after background subtraction. The bare GCE shows the biggest current peak, which could be due to the specific adsorption of AE at the bare GCE electrode surface (curve a). As the GCEs were modified with ssDNA (curve d) and after hybridization with non-complementary sequence (curve c), complementary sequence (curve b), the current peak for the reduction of AE decreased, indicating that the concentration of AE decreased on the surface of the modified GCEs due to the interaction between AE and DNA. The peak currents of AE decreased in the order of bare GCE, complementary sequence, single-base mismatch sequence and ssDNA-modified electrode and the relative standard deviation is 3.20, 6.43, 8.35, and 8.11%, respectively. These results showed that ssDNA was immobilized on the GCE, and complementary sequence was hybridized with the probe ssDNA. When the ssDNA-modified GCE interacted with the complementary sequence in solution, the peak current for the AE increased significantly. This increase in current clearly showed that the ssDNA modified on the GCE had successfully hybridized with its complementary sequence. The greater peak currents indicated that more AE molecules were concentrated or bound to dsDNA helix than to ssDNA helix. The effective discrimination against single-base mismatch was also studied. In the presence of oligonucleotide containing a single-base mismatch, significant decreased voltammetric signal was obtained compared to the complementary sequence. This difference indicates that the complete hybridization was not accomplished due to the base mismatch. In addition, as expected, there was no significant current difference for the ssDNA-modified GCE and its hybridization with non-complementary sequence, since no successful hybridization occured due to the sequence mismatch between the modified ssDNA and the non-complementary sequence. This means that the surface properties of the ssDNA-modified GCE was not changed after its interaction with non-complementary sequence.

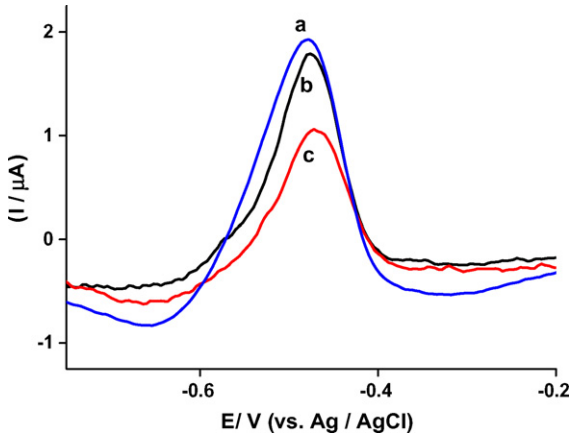

Fig. 6. DPVs responses using the reduction signal of AE for APL probe modified GCE (curve b), APL probe modified GCE after hybridization with negative real sample (curve a), and APL probe modified GCE after hybridization with positive real sample (curve c). Other conditions as Fig. 4.

The sensitivity of the electrochemical hybridization assay was investigated by varying the target oligonucleotide concentration according to the procedure described. The different current value obtained in the DPV response of AE after hybridization of probe with target was recorded with three repetitive measurements. The current response at about −471 mV increased in proportion to the amount of the target sequence used. The average current response showed excellent correlation with the amount of the complementary oligonucleotides applied over the range from 1.5×10^{-8} to 1.5×10^{-7} M. The regression equation was $y = 0.4068x + 3.2729$ (x is the amount of the target DNA (mol) and y is the DPV peak current of AE (μA)) and the regression coefficient of the linear curve were 0.9958. A detection limit of 6.7×10^{-8} M of the target DNA can be estimated using 3σ (where σ is the standard deviation of the blank solution $n = 8$).

Fig. 6 represents the AE signals obtained, when the probe for PML/RARα was immobilized and hybridized with real samples in the hybridization step. A series of three repetitive measurements resulted in reproducible results. The AE signals obtained from the probe modified GCE gave a mean average signal of 2.43 μA with a relative standard deviation (R.S.D.) value of 6.2%. The AE signals obtained from the hybridization of the probe with the positive and negative real samples gave mean average signals of 1.47 μA with a R.S.D. value of 8.9% and 2.60 μA with a R.S.D. value of 7.7%, respectively. The AE signals of the PML/RARα probe modified GCE was higher than that of PML/RARα probe modified GCE after hybridization with positive real sample. The obvious decrease in the magnitude of the AE signals were obtained with positive real samples. The decrease in the voltammetric signals showed that the hybridization at the GCE surface occurred and AE could not interact with the bound guanine base of the hybrid. The decrease in the reduction signal of AE was attributed to the steric inhibition of the reducible groups of AE because of the formation of hybrid at the GCE surface. If the blood sample, from which DNA was extracted, were negative, the negative real sample would not contain a target sequence complementary to the specific PML/RARα probe. The interaction between these negative real samples and the immobilized probe did not lead to the hybridization, so the magnitude of the AE signal was nearly as high as the probe signal (Fig. 6).

4. Conclusions

The interaction between AE and salmon sperm DNA was studied using cyclic voltammetry and differential pulse voltammetry. All the experimental results indicate that the binding mode of AE–DNA is intercalative. In addition, the calculated electrochemical parameters transfer coefficient α and standard electron transfer rate constant k_s reveal that the interaction of AE with DNA forms a nonelectroactive supramolecular complex. The Langmuir adsorption constants of AE at a bare GCE, ssDNA/GCE and dsDNA/GCE were also calculated. The difference in binding constants of AE to ss- and dsDNA suggests that AE can be used as an electrochemical indicator for preparation of DNA hybridization biosensor with a detection limit of 6.7×10^{-8} M, which has been evidenced by the hybridization recognition of immobilized single-stranded PML-RARα fusion gene fragment to its complementary DNA fragment. The utility of AE as an electrochemical hybridization indicator for detection of PML-RARα fusion gene in acute promyelocytic leukemia can provide a simple, rapid detection and might have a promising future in transducing DNA hybridization. The electrochemical DNA sensor developed might have the potential application in diagnosis of diseases.

Acknowledgments

The authors gratefully acknowledge the financial support of the National High Technology and Development of China (863 Project: 2006AA02Z4Z1), the National Natural Science Foundation of China (20675015), the Foundation of Fujian Provincial Technology International Cooperation (2006I0016) and the Foundation of Fujian Education Department (2005K051) and the Foundation of Fujian Health Department (2005123).

References

[1] X.M. Li, H.O. Ju, C.F. Ding, S.S. Zhang, Anal. Chim. Acta 582 (2007) 158.
[2] C.S. Riccardi, K. Dahmouche, C.V. Santilli, P.I. Costa, H. Yamanaka, Talanta 70 (2006) 637.
[3] J. Yang, T. Yang, Y. Feng, K. Jiao, Anal. Biochem. 365 (2007) 24.
[4] E. Komarova, M. Aldissi, A. Bogomolova, Biosens. Bioelectron. 21 (2005) 182.
[5] C. Carrasco, A. Joubert, C. Tardy, N. Maestre, M. Cacho, M.F. Brana, C. Bailly, Biochemistry 42 (2003) 11751.
[6] A. Erdem, M. Ozsoz, Anal. Chim. Acta 437 (2001) 107.
[7] X.H. Lin, P. Wu, W. Chen, Y.F. Zhang, X.H. Xia, Talanta 72 (2007) 468.
[8] B. Meric, K. Kerman, D. Ozkan, P. Kara, S. Erensoy, U.S. Akarca, M. Mascini, M. Ozsoz, Talanta 56 (2002) 837.
[9] K. Maruyama, Y. Mishima, K. Minagawa, J. Motonaka, Anal. Chem. 74 (2002) 3698.
[10] S.S. Zhang, S.Y. Niu, B. Qu, G.F. Jie, H. Xu, C.F. Ding, J. Inorg. Biochem. 99 (2005) 2340.
[11] X. Zhou, S. Zheng, D. Li, X. He, B. Lin, Talanta 72 (2007) 561.

[12] Y.Q. Li, Y.J. Guo, X.F. Li, J.H. Pan, Talanta 71 (2007) 123.
[13] A.M. Pyle, J.P. Rehmann, R. Meshoyrer, C.V. Kumar, N.J. Turro, J.K. Barton, J. Am. Chem. Soc. 111 (1989) 3051.
[14] F. Yang, T. Zhang, G. Tian, H. Cao, Q. Liu, Y. Ito, J. Chromatogr. A 858 (1999) 103.
[15] K.E. Malterud, T.L. Farbrot, A.E. Huse, R.B. Sund, Pharmacology 47 (1993) 77.
[16] H.Z. Lee, S.L. Hsu, M.C. Liu, C.H. Wu, Eur. J. Pharmacol. 43 (2001) 1287.
[17] S.O. Muller, H. Stopper, Biochim. Biophys. Acta 1428 (1999) 406.
[18] H.H. Wang, J.G. Chung, C.C. Ho, L.T. Wu, S.H. Chang, Planta Med. 64 (1998) 176.
[19] R.E. McKnight, J.G. Zhang, D.W. Dixon, Bioorg. Med. Chem. Lett. 14 (2004) 401.
[20] S. Bi, D. Song, Y. Kan, D. Xu, Y. Tian, X. Zhou, H. Zhang, Spectrochim. Acta A 62 (2005) 203.
[21] A. Laurenzana, F. Pettersson, W.H. Miller Jr, Drug Discov. Today 3 (2006) 499.
[22] E. Paietta, O. Goloubeva, D. Neuberg, J.M. Bennett, R. Gallagher, J. Racevskis, G. Dewald, P.H. Wiernik, M.S. Tallman, Eastern Cooperative Oncology Group, Cytometry B Clin. Cytom. 59 (2004) 1.
[23] R. He, B. Liu, C. Yang, R.C. Yang, G. Tobelem, Z.C. Han, Cancer Gene Ther. 10 (2003) 879.
[24] J. Chen, J. Zhang, Q. Zhuang, S. Zhang, X. Lin, Talanta 72 (2007) 1805.
[25] L. Tan, S. Yao, Q. Xie, Talanta 71 (2007) 827.
[26] A.J. Bard, L.R. Faulkner, Electrochemical Methods Fundamentals and Applications, Wiley, New York, 1980, pp. 166.
[27] E. Laviron, J. Electroanal. Chem. 101 (1979) 19.
[28] X. Zheng, A. Chen, T. Hoshi, J.I. Anzai, G. Li, Anal. Bioanal. Chem. 386 (2006) 1913.
[29] E.C. Long, J.K. Barton, Acc. Chem. Res. 23 (1990) 271.
[30] Y.F. Long, C.Z. Huang, Talanta 71 (2007) 1939.
[31] Z. Sun, Z. Ma, W. Zhang, X. Wang, C. Fan, G. Li, Anal. Bioanal. Chem. 379 (2004) 283.
[32] H. Zhou, Z.Y. Sun, T. Hoshi, Y. Kashiwagi, J.I. Anzai, G. Li, Biophys. Chem. 114 (2005) 21.
[33] H.X. Ju, Y.K. Ye, Y.L. Zhu, Electrochim. Acta 50 (2005) 1361.